Journal of Computing and Electronic Information Management
ISSN: 2413-1660 | Vol. 19, No. 2, 2025

Analysis of Magnetic Bearing Magnetic Field Based on Subdomain Model

Kai Li [1], Xiaohu Wang [1], Teng Hu [1,*], Guilin Li [2] and Yanjun Li [3]

[1] School of Mechanical Engineering, Southwest Petroleum University, Chengdu 610500, China
[2] Taihang National Laboratory, Chengdu 610200, China
[3] AECC Sichuan Gas Turbine Establishment, Chengdu 610500, China

*** Corresponding author**

Abstract: Precise electromagnetic field analysis is essential for optimizing the performance of magnetic bearings in high-speed rotating machinery. To overcome the computational inefficiencies associated with Finite Element Analysis (FEA), this paper proposes an exact analytical technique based on the subdomain model for radial magnetic bearings. The magnetic domain is partitioned into stator slot and air gap subregions, where Poisson's and Laplace's equations are solved, respectively, under the assumption of infinite permeability of the iron core. By satisfying the continuity conditions of magnetic vector potential and magnetic field intensity at the subregion interfaces, the general solutions for the magnetic field distribution are derived. Additionally, the model accounts for the influence of rotor eccentricity on the air gap flux density. The proposed analytical method is validated through comparison with FEA simulations under various operating conditions, including different bias currents and eccentricity angles. The results demonstrate that the subdomain model achieves high accuracy in predicting flux density while significantly reducing computational time, confirming its viability for the efficient design of active magnetic bearing systems.

Keywords: Magnetic Bearing; Subdomain Model; Electromagnetic Field.

1. Introduction

Magnetic bearings are crucial in high-speed rotating machinery due to their contactless operation, minimal friction, and increased longevity, making them suitable for applications in turbines, compressors, and energy storage systems (0). Precise electromagnetic field analysis in these bearings is vital for optimizing levitation forces, system stability, and control strategies, directly impacting overall performance and efficiency [1]. While finite element analysis (FEA) offers detailed simulations, it is often computationally demanding, leading to the adoption of analytical methods for quicker and more efficient modeling [2]. The subdomain model method stands out as an effective analytical approach, partitioning the magnetic domain into subregions like air gaps, magnets, and ferromagnetic components, where Laplaces or Poissons equations are solved independently under matching boundary conditions to derive exact magnetic field distributions [3]. This technique is particularly adept at managing complex geometries and heteropolar setups in radial magnetic bearings, facilitating accurate predictions of flux density, forces, and torques with reduced computational resources [4]. Recent developments have applied the subdomain method to solid-rotor configurations, enhancing models for eddy currents and rotor eccentricities [5]. Validation through experiments confirms the methods reliability in axial and radial active magnetic bearings, especially in multi-degree-of-freedom platforms [6]. Moreover, combining it with perturbation techniques extends its utility to dynamic analyses, such as vibration mitigation in high-speed environments [7]. Additional studies on isolated and hybrid active magnetic bearings further demonstrate its versatility in handling saturation effects and distributed modeling [8].

2. Electromagnetic Field Subdomain model

2.1. Basic Assumptions

For the magnetic bearing stator, the primary subjects of analysis for the electromagnetic field subdomain model are the stator slots and the air gap. All other parameters are consistent with those in the temperature field analysis, as shown in Fig. 1. To establish the electromagnetic field subdomain model, the following basic assumptions are made:

The relative permeability of the bearing material is assumed to be infinite.

1) Eddy current effects are ignored.
2) The electromagnetic field is uniformly distributed along the axial direction.

These assumptions are widely adopted in semi-analytical modeling studies of radial magnetic bearings and similar electrical machines, as they preserve the tractability of the analytical solution while capturing the key physical phenomena.

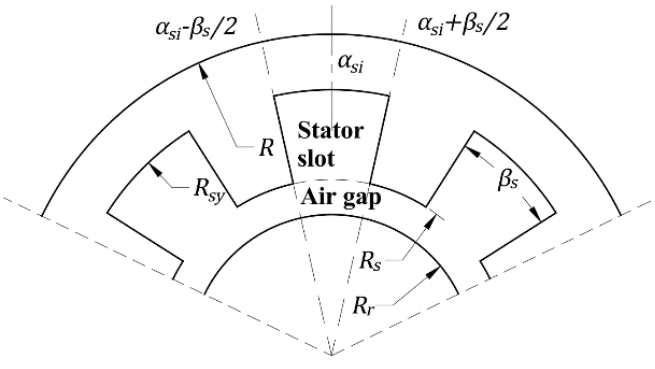

Fig. 1 Basic structure of magnetic bearing stator

2.2. Air Gap Region

There is no excitation current in the air gap region, therefore, it is described by the Laplace equation:

$$\begin{cases} \dfrac{\partial^2}{\partial r^2}A_g(r,\theta)+\dfrac{1}{r}\dfrac{\partial}{\partial r}A_g(r,\theta)+\dfrac{1}{r^2}\dfrac{\partial^2}{\partial \theta^2}A_g(r,\theta)=0 \\ 0<\theta<2\pi, R_r<r<R_s \end{cases} \quad (1)$$

From (1), the distribution equation for the magnetic vector potential, $A_g(r,\theta)$, in the air gap region can be obtained:

$$A_g(r,\theta)=D_0+E_0 lnr+\sum_{n=1}^{\infty}\left(C_{1n}r^n+C_{2n}r^{-n}\right)\sin(n\theta)+\sum_{n=1}^{\infty}\left(C_{3n}r^n+C_{4n}r^{-n}\right)\cos(n\theta) \quad (2)$$

According to Amperes circuital law, for any circular closed path centered at the origin with a radius $R_r < r < R_s \mathrm{R_r} < \mathrm{r} < \mathrm{R_s}$, we have:

$$\oint B_g dl=-2\pi E_0=\mu_0 I_e \quad (3)$$

In the equation, μ_0 is the vacuum permeability, I_e is the total current enclosed by the path. Since there is no excitation current in either the air gap or the rotor, I_e is 0 which means $E_0 = 0$. Thus, the equation becomes:

$$A_g(r,\theta)=D_0+\sum_{n=1}^{\infty}\left(C_{1n}r^n+C_{2n}r^{-n}\right)\sin(n\theta)+\sum_{n=1}^{\infty}\left(C_{3n}r^n+C_{4n}r^{-n}\right)\cos(n\theta) \quad (4)$$

Here, D_0 is the undetermined constant coefficient; C_{1n}, C_{2n}, C_{3n} and C_{4n} are the undetermined coefficients of the series terms; and n is the summation index for the air gap region.

2.3. Stator Slot Region

An excitation current exists in the stator slots. Assuming its current density is J, the region is described by the Poisson equation:

$$\begin{cases} \dfrac{\partial^2}{\partial r^2}A_s(r,\theta)+\dfrac{1}{r}\dfrac{\partial}{\partial r}A_s(r,\theta)+\dfrac{1}{r^2}\dfrac{\partial^2}{\partial \theta^2}A_s(r,\theta)=-\mu_0 J \\ \alpha_{si}-\dfrac{\beta_s}{2}<\theta<\alpha_{si}+\dfrac{\beta_s}{2}, R_s<r<R_{sy} \end{cases} \quad (5)$$

The boundary conditions for the left and right sides of the stator slot are:

$$\frac{\partial A_s(r,\theta)}{\partial \theta}\Big|_{\theta=\alpha_{si}-\frac{\beta_s}{2}}=0 \quad (6)$$

$$\frac{\partial A_s(r,\theta)}{\partial \theta}\Big|_{\theta=\alpha_{si}+\frac{\beta_s}{2}}=0 \quad (7)$$

The boundary condition for the top of the stator slot is:

$$\frac{\partial A_s(r,\theta)}{\partial r}\Big|_{r=R_{sy}}=0 \quad (8)$$

By solving the Poisson equation in (5) and substituting the boundary conditions in (6), (7) and (8), the distribution equation for the magnetic vector potential in the stator slot region, $A_s(r,\theta)$, can be obtained:

$$A_s(r,\theta)=F_0+\frac{1}{2}\mu_0 J R_{sy}^2 lnr-\frac{1}{4}\mu_0 J r^2+\sum_{k=1}^{\infty}D_k\left(r^{\frac{k\pi}{\beta_s}}+R_s^{\frac{2k\pi}{\beta_s}}r^{-\frac{k\pi}{\beta_s}}\right)\cos\left(\frac{k\pi}{\beta_s}\left(\theta-\alpha_{si}+\frac{\beta_s}{2}\right)\right) \quad (9)$$

Here, F_0 is the undetermined constant coefficient, D_k is the undetermined coefficient of the series terms, and k is the summation index for the stator slot region.

2.4. The Solution of Subdomain Method

At the interface between the stator slots and the air gap, the magnetic vector potential continuity condition must be satisfied:

$$\begin{cases} A_g(r,\theta)|_{r=R_s}=A_s(r,\theta)|_{r=R_s} \\ \alpha_{si}-\dfrac{\beta_s}{2}<\theta<\alpha_{si}+\dfrac{\beta_s}{2} \end{cases} \quad (10)$$

The magnetic field intensity must also be continuous:

$$\begin{cases} \dfrac{\partial A_g(r,\theta)}{\partial r}|_{r=R_s}=\dfrac{\partial A_s(r,\theta)}{\partial r}|_{r=R_s} \\ \alpha_{si}-\dfrac{\beta_s}{2}<\theta<\alpha_{si}+\dfrac{\beta_s}{2} \end{cases} \quad (11)$$

By simultaneously solving these equations, the values for each undetermined coefficient can be obtained, which allows for solving $A_g(r,\theta)$ and $A_s(r,\theta)$. The magnetic flux density in the air gap region can then be calculated with the following formulas:

$$\begin{cases} B_{gr}(r,\theta)=\dfrac{1}{r}\dfrac{\partial}{\partial \theta}A_g(r,\theta) \\ B_{gt}(r,\theta)=-\dfrac{\partial}{\partial r}A_g(r,\theta) \end{cases} \quad (12)$$

Here, $B_{gr}(r,\theta)$ is the radial component of the flux density and $B_{gt}(r,\theta)$ is the tangential component. The total flux density in the air gap is written as:

$$B_g(r,\theta)=\sqrt{B_{gr}(r,\theta)^2+B_{gt}(r,\theta)^2} \quad (13)$$

2.5. Rotor Eccentricity

When rotor eccentricity is present, it is necessary to consider not only the dimensional changes caused by thermal expansion but also to superimpose the changes in air gap size caused by the eccentricity for each pole pair. Without considering thermal expansion, the air gap size with an eccentric rotor is given by:

$$x_0'(\theta)=x_0-e\cos(\theta-\gamma) \quad (14)$$

Where e is the rotor eccentricity distance, and γ is the rotor eccentricity angle.

The resulting air gap flux density, $B_g'(r,\theta)$, is calculated with the formula:

$$B_g'(r,\theta)=\frac{x_0 B_g(r,\theta)}{x_0-x_0 e\cos(\theta-\gamma)+x_i} \quad (15)$$

3. Verification of Results

The calculation results of the electromagnetic field subdomain model are verified using the relevant parameters from Table 1.

Fig. 2 and Fig. 3 show a comparison between the subdomain models calculated air gap flux density and the results from the Finite Element Method under maximum load conditions. The simulations use 160 coil turns with bias currents I_b of 1 A and 1.5 A, respectively.

Table .1 Main Parameters of Magnetic Bearing

Parameters	Value
Stator outer radius R	80 mm
Stator yoke radius R_{sy}	60 mm
Stator inner radius R_s	37.5 mm
Rotor outer radius R_r	37 mm
Pole height L_1	11.25 mm
Bearing thickness L_2	20 mm
Number of poles N_s	8
Stator slot opening angle β_s	25 °
Pole arc angle β_p	20 °
Material thermal conductivity k_s	44.5 W/m·K
Material Poissons ratio ν	0.28
Coil resistivity ρ	1.6e-8 Ω·m
Bare wire diameter ϕ	0.8 mm

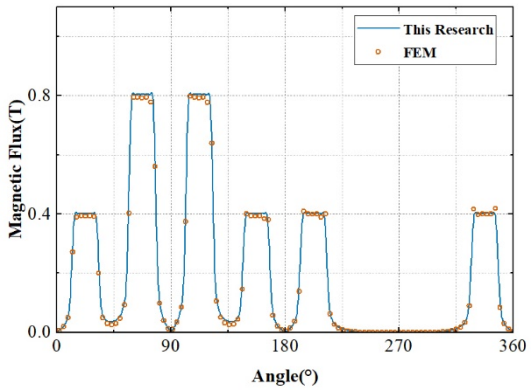

Fig. 2 1 A bias current 160 turns, maximum load, air gap flux density calculation results.

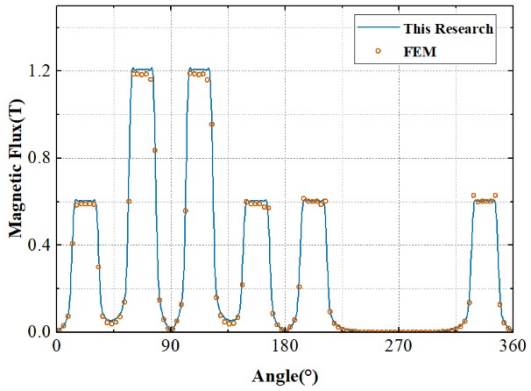

Fig. 3 1.5 A bias current 160 turns, maximum load, air gap flux density calculation results.

Keeping the previous conditions constant and setting the eccentricity ratio ϵ to 0.3, the air gap flux density distributions for different eccentricity angles are compared with the finite element results, as shown in Fig.4.

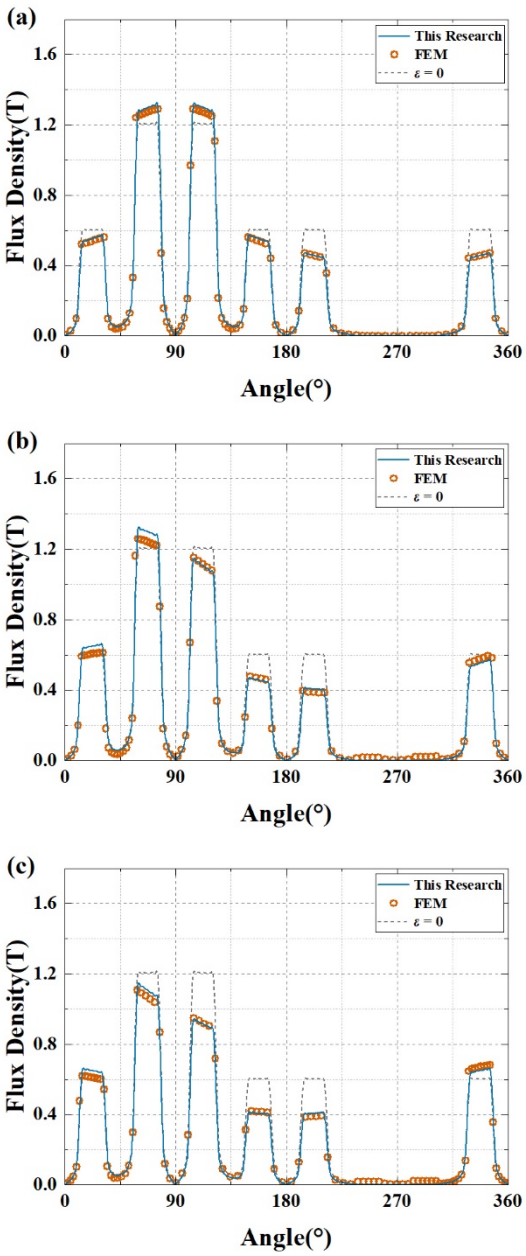

Fig. 4 Flux density in air gap at different eccentricity angle. (a) $\gamma = 90$ °. (b) $\gamma = 135$ °. (c) $\gamma = 180$ °.

4. Summary

This study proposes an analytical approach based on the subdomain model for the precise and efficient analysis of the electromagnetic field in radial magnetic bearings, addressing the high computational demands of Finite Element Analysis (FEA). The magnetic domain is partitioned into stator slot and air gap subregions. Under the assumptions of infinite core permeability and negligible eddy current effects, the model independently solves Poissons and Laplaces equations within these regions.

By enforcing continuity conditions for the magnetic vector potential and magnetic field intensity at the interfaces, the authors derive exact analytical solutions for the magnetic field distribution, including calculations for conditions involving rotor eccentricity. To validate the model, the analytical calculations were compared with FEA simulation results. The study confirms a high degree of consistency in the air gap flux density distribution under maximum load conditions and at various rotor eccentricity angles. These results demonstrate

that the subdomain model effectively predicts the electromagnetic characteristics of magnetic bearings while significantly reducing computational resource requirements compared to FEA.

Acknowledgements

This work was supported by Taihang National Laboratory of China (A2063).

References

[1] Yu, C., Deng, Z., Chen, S., et al. A novel subdomain and magnetic circuit modeling method for hybrid homopolar radial magnetic bearings. Mechanical Systems and Signal Processing. 2022, Vol. 170, p. 108823.

[2] Sikora, B. M., Piłat, A. K. Analytical modeling and experimental validation of the six pole axial active magnetic bearing. Applied Mathematical Modelling. 2022, Vol. 104, p. 50-66.

[3] Yang, F., Zhao, Y., Li, H., et al. Design and Analysis of a 2-DOF Electromagnetic Actuator with an Improved Halbach Array for the Magnetic Suspension Platform. Sensors. 2022, Vol. 22 (No. 3), p. 790.

[4] Dutta, D., Debnath, S., Biswas, P. K. Exact analytic technique for designing controller architecture in multi-axis active magnetic bearings with rotor eccentricities. Mechanics Based Design of Structures and Machines. 2025, Vol. 53 (No. 5), p. 3823-3841.

[5] Wang, K., Wang, D., Shen, Y., et al. Subdomain Method for Permanent Magnet Biased Homo-Polar Radial Magnetic Bearing. IEEE Transactions on Magnetics. 2016, Vol. 52, p. 1-5.

[6] Yu, C., Wang, T., Shi, Y., Ren, X. Accurate modelling based on a subdomain method for heteropolar radial magnetic bearing with a solid rotor. IET Electric Power Applications. 2021, Vol. 15 (No. 6), p. 747-760.

[7] Ren, X., Wang, T., Yu, C., Shi, Y. Magnetic field analytical calculation method for radial unite of a combined magnetic bearing. IET Electric Power Applications. 2023, Vol. 17 (No. 3), p. 402-414.

[8] Du, T., Geng, H., Zhang, Y., et al. Exact Analytical Method for Active Magnetic Bearings With Rotor Eccentricity. IEEE Transactions on Magnetics. 2019, Vol. 55 (No. 12), p. 1-12.